Modelling of anti-inflammatory treatment in the Alzheimer disease: optimal regimen and outcome

W. El Hajj*[1], L. Pujo-Menjouet[1], L. M. Tine[1], and V. Volpert[1,2]

[1] *Universite Claude Bernard Lyon 1, CNRS, Centrale Lyon, INSA Lyon, Université Jean Monnet, ICJ UMR5208, 69622 Villeurbanne, France.*

[2] *Peoples' Friendship University of Russia (RUDN University), 6 Miklukho-Maklaya St, Moscow 117198, Russian Federation*

October 16, 2025

Abstract

The application of non-steroidal anti-inflammatory drugs (NSAIDs) for Alzheimer's disease is considered to be a promising therapeutic approach. Epidemiological studies suggest potential benefits of NSAIDs; however, these findings are not consistently supported by clinical trials. This long-standing discrepancy has persisted for decades and remains a significant barrier to developing effective treatment strategies. To assess the efficacy of NSAIDs in Alzheimer's disease, we have developed a mathematical model based on a system of ordinary differential equations. The model captures the dynamics of key players in disease progression, including Aβ-monomers, oligomers, pro-inflammatory mediators (M1 microglial cells and pro-inflammatory cytokines), and anti-inflammatory mediators (M2 microglial cells and anti-inflammatory cytokines). The effects of NSAIDs are modeled through a reduction in the production rate of inflammatory cytokines (IC). While a single NSAID administration temporarily reduces IC levels, their concentration eventually returns to baseline due to drug elimination. The return time depends on the drug dose, resulting in a patient-specific return time function. By analyzing this function, we propose an optimal treatment regimen and identify conditions under which NSAID treatment is most effective in reducing IC levels. Our results suggest that NSAID efficacy in Alzheimer's disease is influenced by the stage of the disease (with earlier intervention being more effective), patient-specific parameters, and the treatment regimen. The approach developed here can also be generalized to evaluate the efficacy of anti-inflammatory treatments for other diseases.

Keywords: Alzheimer's diseases, inflammation, anti-inflammatory treatment, NSAID

1 Introduction

1.1 Biological background

According to the latest statistical reports, around 57.4 million of people are living with Alzheimer's diseases (AD) globally and this number is expected to increase to 152.8 million in 2050 [1]. AD is a progressive

*Corresponding author: elhajj@math.univ-lyon1.fr

neurodegenerative disease that affects cognitive abilities. It is linked to the misfolding, aggregation and accumulation of various proteins within the nervous system [2, 3]. These proteins form stable oligomers, one of them is Aβ, which are considered to be the cause of progressive and irreversible damage to neurons [4, 5]. Neurons produce Aβ-monomers that undergo polymerization to become proto-oligomers. Proto-oligomers polymerize and depolymerize until reaching a critical size, they become stable under the form of Aβ-oligomers. Under such form, oligomers cannot undergo polymerization nor depolymerization [6, 7, 8] and are considered cytotoxic [9]. The latter mechanism involving the misfolding of Aβ-oligomers is referred to as the amyloid cascade hypothesis [10], and it plays a major role in the progression of Alzheimer's disease (AD) [2, 8]. The presence of cytotoxic Aβ-oligomers in the brain leads to the set-up of an immune response by the activation of microglial cells, as shown in Figure 1. Microglia are immune cells of the central nervous system that regulate brain development and injury repair. Microglia activation is an important stage of inflammation leading to the production of pro-inflammatory cytokines (such as TNF-α, IL-1) [11]. The release of pro-inflammatory cytokines up-regulates the production of Aβ-monomers [12].

During neuroinflammation, the interplay between pro-inflammatory and anti-inflammatory pathways coordinates the dynamics of immune responses in the brain (Figure 1). We distinguish two phenotypes of activated microglial cells, namely M1 and M2 phenotypes. M1 activated microglia are considered pro-inflammatory because they promote the development of inflammation by producing pro-inflammatory cytokines, causing the death of neurons [13]. They also interact with astrocytes leading them to produce neurotoxic factors and to decrease phagocytic activity [14]. In contrast, M2 microglia produce anti-inflammatory cytokines such as IL-10 and transforming growth factor (TGF-β) [15]. They promote phagocytosis of cell debris and misfolded proteins, inhibit the production of pro-inflammatory agents, and support neuron survival [16]. Some studies have shown the primary role of neuroinflammation in the process of Alzheimer's disease revealing the alteration in the levels of cytokines in AD patients [17, 18]. For example, increased TNF-α is a key element in inflammatory cascade and increases the Aβ-monomer production [19]. Moreover, it has been shown that short-term anti-TNF-α treatment improves cognition in AD patients [20]. The role of the anti-inflammatory cytokine IL-4 is important in neutralizing the neuroinflammatory process in AD brains. Some in vivo experiments show that IL-4 reduces the accumulation of non-plaque forms of Aβ-proteins [21]. However, AD patients show a decrease in the concentration of IL-4 leading to an imbalance between pro- and anti-inflammatory cytokines which accelerate the AD process [18].

Inflammation plays a major role in the progression of the diseases and several therapeutic strategies are implemented to attenuate the negative effect of AD. For example, non-steroidal anti-inflammatory drugs (NSAIDs) are medicines that are widely used as a treatment for fever, pain and inflammation. Several epidemiological studies show that NSAIDs can be considered as neuroprotective since they target microglia, major contributors to neurodegeneration [22, 23, 24]. For example, diclofenac-based drugs might be associated with slower cognitive decline [25]. Furthermore, some studies have suggested that, if started early enough, a daily regimen of the non-prescription NSAID ibuprofen can prevent the onset of Alzheimer's disease [26]. Although this type of drugs crosses the blood brain barrier (BBB) efficiently, the dose reaching the brain is different due to many neuropathological conditions [27]. The effect of such drugs on microglial functions consists in the inhibition of COX activity (cyclooxygenase enzymes involved in inflammation) [23], in down-regulation of the expression of genes responsible for activating inflammatory pathways (NF-κB) [28] and activating PPAR-γ (nuclear receptor) [29]. Several studies show that PPAR-γ control brain inflammation and is highlighted as a promising therapeutic use in human brain diseases.

Though epidemiological studies support the evidence that the use of NSAID reduces the risk of AD [25, 27, 30], clinical studies have not confirmed that NSAID has a positive effect on the Alzheimer patients. Some possible explanations for such discrepancy is that NSAID can only be effective in early stages of

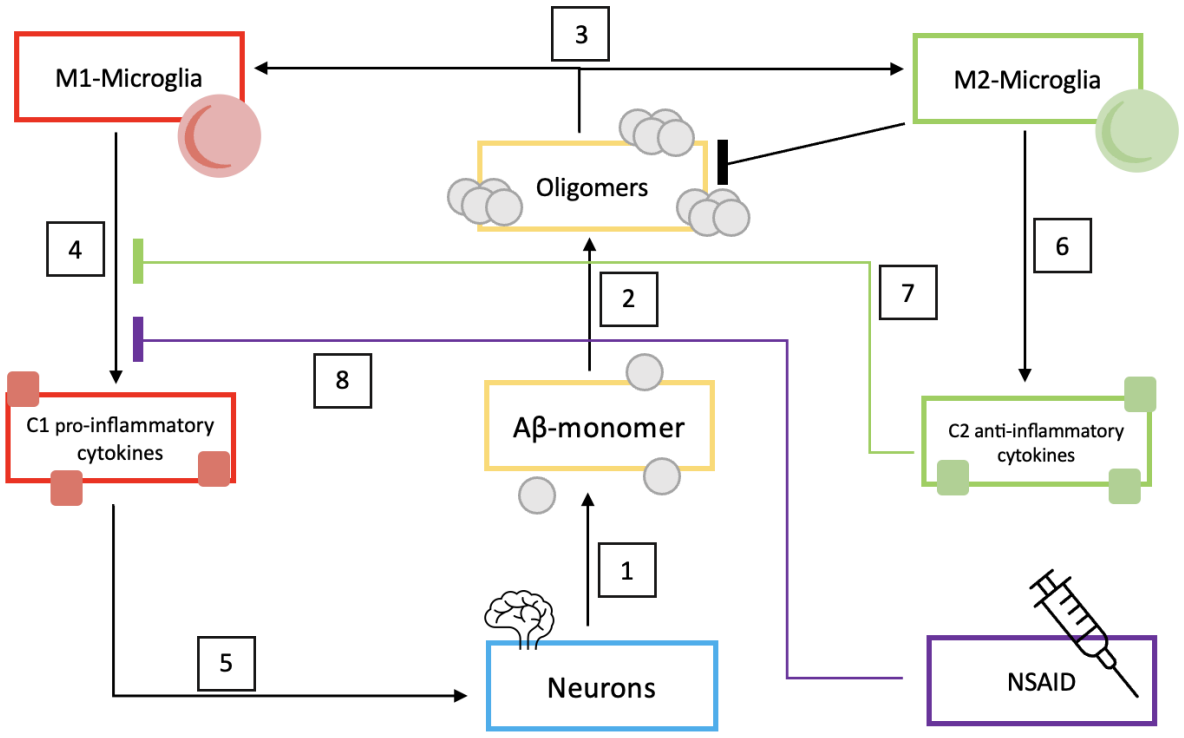

Figure 1: Scheme depicting the biological phenomena of Aβ-monomers and inflammation including neurons, Aβ-monomers, oligomers, M1-M2 microglial cells, C1-C2 inflammatory cytokines and non-steroidal anti-inflammatory drugs (NSAID). Neurons produce Aβ-monomers (1) that polymerize into stable oligomers (2). Stable oligomers activate microglial cells (3) that causes the set-up of an inflammatory response by producing inflammatory cytokines. M1 type microglia produce C1 pro-inflammatory cytokines (4) that in return stimulate neurons (5) to produce additional Aβ-monomers. In contrast, M2 type microglia produce C2 anti-inflammatory cytokines (6) and eliminates oligomers. Anti-inflammatory cytokines (7) and NSAID (8) inhibit the production of pro-inflammatory cytokines.

the disease and is non-beneficial for later stages [22, 25, 30] or that the concentration of NSAID reaching the brain is not sufficient because of the blood-brain barrier. Furthermore, such type of drugs require a prolonged period of administration in order to provide a protective effect [31].

In this work we use mathematical modelling in order to study whether NSAID treatment can be beneficial for virtual patients and to determine the optimal treatment regimen.

1.2 Mathematical modeling of Alzheimer disease in the literature

During the last decades, several studies were devoted to the onset of AD [32] and the role of prions interacting with Aβ [33]. In [32], the authors propose a system of transport and diffusion equation to study the set-up and the progression of the disease with a focus on the diffusion and removal of Aβ. They study the spread of neuronal damage at different stages of the disease evolution and particularly the cerebral damage at the early stages.

Mathematical models study the interactions between key components in the brain, including oligomers [34] and Aβ-plaques [35], emphasizing their roles in disease progression. For example, authors in [34]

suggest a model to study the spatial propagation of amyloid-beta (Aβ) oligomers in the early stages of AD. Numerical simulations are used to study the balance between oligomers diffusion and replication, and show that fragmentation rate of oligomers considerably affects their neurotoxic effects on the progression of the disease. Authors in [35] propose a model based on macroscopic integro-differential equations to study the interplay between amyloid-beta and tau proteins in the development of AD. Through transport and diffusion equations, they highlight that Aβ and tau interactions significantly impact the disease distribution in the brain at early and advanced stages of the disease. Moreover, they showed that the removal of toxic Aβ from the cerebrum promotes tissue regeneration.

Inflammation processes plays a crucial role in the progression of AD. Hence, some studies are devoted to investigate the role of inflammatory processes, namely the activation of microglial cells [36], the role of pro-inflammatory cytokines [37] and the anti-inflammatory effect [38, 39]. In [36] the authors present a system of ordinary differential equations modeling the interaction between seven key-players of the disease such as neurons, Aβ and microglial cells. They highlight that inflammatory activation of resting microglial cells is a crucial step for progressive neuron death and should be further studied. The work [37] suggests a spatially homogeneous system of equations to study the interactions between monomers, oligomers, microglial cells and pro-inflammatory cytokines. It is shown that inflammation can trigger the disease through a hysteresis effect, where disease development or remission depend on the degradation rate of oligomers. Furthermore, they discuss some perspectives of anti-inflammatory treatments of AD. Similarly, authors in [39] suggest that some anti-inflammatory drug therapy could slow the development of the disease. They develop a system of partial differential equations describing the interactions between neurons, microglias, tumor necrosis factor alpha TNF-α and anti-inflammatory cytokines. Through numerical simulations, they assess the efficacy of TNF-α inhibitor and anti-amyloid β as a possible therapy.

In this work, we propose a mathematical model describing Aβ production, inflammation and effect of NSAID (Section 1.3). The proposed model describes the pro- and anti-inflammatory aspects in the case of Alzheimer disease. We begin with the analysis of the existence of solutions, existence of stationary points and their stability (Section 2). Then, we focus on the role of NSAID in the inflammation progression for a simplified model (Section 3) and subsequently for the complete model (Section 4). The main objective of this work is to elucidate why a NSAID treatment may not be efficient in some cases and to propose an optimal treatment regimen.

1.3 Mathematical model

In this section, we present a mathematical model describing Aβ production and inflammation, as shown in Figure 1. The model consists of an ordinary differential system of equations for the concentrations Aβ-monomers, Aβ-proto-oligomers of size i, Aβ-oligomers, M1 pro-inflammatory microglial cells, pro-inflammatory cytokines, M2 anti-inflammatory microglial cells and anti-inflammatory cytokines.

Proto-oligomers and oligomers production. Abnormal amyloid-β is produced by activated neurons, and form proto-oligomers and oligomers. The concentration of neurons N is considered to be constant. Their death can be neglected in the beginning of AD. In the later stages, when they start to die, their concentration can be considered as quasi-stationary since it is a slow process in the time scale of inflammation processes. We denote the amyloid-β concentration by A and the concentration of proto-oligomers of length i by u_i. We do not take into account the process of depolymerization of proto-oligomers. We fix $n \in \mathrm{N}$, the maximal size of proto-oligomers by polymerization, meaning they can no longer undergo either polymerization or depolymerization [6, 7, 8]. Then, their concentrations are described by the system of equations

$$\frac{dA}{dt} = k_1 C_1 N - 2k_2 A^2 - \sigma_1 A - \sum_{i=2}^{n} r_i A u_i, \tag{1.1}$$

$$\frac{du_2}{dt} = k_2 A^2 - r_2 A u_2 - \sigma_2 u_2 (1 + bM_2), \tag{1.2}$$

$$\frac{du_3}{dt} = r_2 A u_2 - r_3 A u_3 - \sigma_2 u_3 (1 + bM_2), \tag{1.3}$$

$$\frac{du_i}{dt} = r_{i-1} A u_{i-1} - r_i A u_i - \sigma_2 u_i (1 + bM_2), \quad i \in \{2, \cdots, n-1\} \tag{1.4}$$

$$\frac{du_n}{dt} = r_{n-1} A u_{n-1} - \sigma_2 u_n (1 + bM_2), \tag{1.5}$$

The first term in the right-hand side of equation (1.1) describes production of abnormal amyloid-β under the influence of inflammatory cytokines C_1. For simplicity, production of normal amyloid without inflammation is not taken into consideration. The second term in equation (1.1) characterizes aggregation of two molecules leading to production of u_2 proto-oligomers, and the third term represent the natural degradation rate of amyloid-β. The last term in equation (1.1) represents the polymerization of one monomer with a proto-oligomer of size i to form an oligomer of size $i+1$. We denote by r_i, $i \in \{2, ..., n\}$, the polymerization rate. Equation (1.2) describes the evolution in time of the concentration of u_2 proto-oligomers. The first term in the right-hand side of this equation represents the production of u_2 from A and the second term corresponds to the polymerization of an proto-oligomer of size 2. The last term in equation (1.2) characterizes the degradation and elimination of u_2 by activated microglia cells M_2. Similar terms are present in the next equations. For simplicity of presentation, we assume that n can take any large value.

For simplification, we consider that the length of proto-oligomers, n, is sufficiently large so that we can set u to be the sum of all size of proto-oligomers i for $i \in \{2, ..., n\}$. We set $u = \Sigma_{i=2}^{n} u_i$, and take a sum of equations (1.2)-(1.5), we obtain

$$\frac{du}{dt} = k_2 A^2 - \sigma_2 u (1 + bM_2). \tag{1.6}$$

For simplicity, we denote by u the concentration of oligomers. In fact, we consider a bi-monomeric nucleation as used in [37]. We assume that two monomers can merge to form a free oligomer ($A + A \to u$) and the intermediate proto-oligomer phase is neglected. Therefore, equations (1.1) and (1.6) become:

$$\frac{dA}{dt} = k_1 C_1 N - 2k_2 A^2 - \sigma_1 A, \tag{1.7}$$

$$\frac{du}{dt} = k_2 A^2 - \sigma_2 u (1 + bM_2). \tag{1.8}$$

Microglia activation. Microglia phenotype M_1 are activated by oligomers u:

$$\frac{d\tilde{M}_1}{dt} = -k_3 u \tilde{M}_1, \tag{1.9}$$

$$\frac{dM_1}{dt} = k_3 u \tilde{M}_1 - \sigma_3 M_1. \tag{1.10}$$

Here $\tilde{M}_1$ is the concentration of inactive microglia and M_1 the concentration of activated microglia. The last term of equation (1.10) corresponds to the rate of death or exhaustion. We assume that σ_3 is sufficiently small, then we can use approximate equality $\tilde{M}_1 + M_1 = M_1^0$, where M_1^0 is the initial microglia concentration. Under such assumptions, we exclude $\tilde{M}_1$ and consider the following equation for M_1 microglia:

$$\frac{dM_1}{dt} = k_3 u(M_1^0 - M_1) - \sigma_3 M_1. \tag{1.11}$$

A similar equation is considered for the concentration M_2 of alternatively activated microglia:

$$\frac{dM_2}{dt} = k_6 u(M_2^0 - M_2) - \sigma_5 M_2. \tag{1.12}$$

Cytokine production. Classically activated microglia produce pro-inflammatory cytokines C_1 [13]:

$$\frac{dC_1}{dt} = \frac{k_4 M_1}{1 + k_5 C_2} - \sigma_4 C_1. \tag{1.13}$$

Their production rate is down-regulated by anti-inflammatory cytokines C_2 produced by alternatively activated microglia M_2:

$$\frac{dC_2}{dt} = k_7 M_2 - \sigma_6 C_2. \tag{1.14}$$

The last terms in these equations represent the degradation rate of the corresponding cytokines.

Anti-inflammatory treatment. Non-steroidal anti-inflammatory drugs (NSAIDs) act on COX1, COX2 and other molecules participating in production of inflammatory cytokines. We consider here a simplified pharmacokinetics of the NSAID treatment either with a constant drug concentration or exponentially decreasing in time due to its elimination from the body. We take into account in equation (1.13) that NSAIDs with concentration D down-regulate C_1 production rate, where a denotes the rate of down-regulation:

$$\frac{dC_1}{dt} = \frac{k_4 M_1}{(1 + k_5 C_2)(1 + aD)} - \sigma_4 C_1. \tag{1.15}$$

Resulting model. We obtain the following model:

$$\frac{dA}{dt} = k_1 C_1 N - 2k_2 A^2 - \sigma_1 A, \tag{1.16}$$

$$\frac{du}{dt} = k_2 A^2 - \sigma_2 u(1 + bM_2), \tag{1.17}$$

$$\frac{dM_1}{dt} = k_3 u(M_1^0 - M_1) - \sigma_3 M_1, \tag{1.18}$$

$$\frac{dC_1}{dt} = \frac{k_4 M_1}{(1 + k_5 C_2)(1 + aD)} - \sigma_4 C_1, \tag{1.19}$$

$$\frac{dM_2}{dt} = k_6 u(M_2^0 - M_2) - \sigma_5 M_2, \tag{1.20}$$

$$\frac{dC_2}{dt} = k_7 M_2 - \sigma_6 C_2. \tag{1.21}$$

In general, the drug concentration is a function of time, $D = D(t)$. We describe the evolution in time for D by the equation

$$\frac{dD}{dt} = -kD. \tag{1.22}$$

Equation (1.22) states that the concentration of NSAID decreases with time due to its elimination from the body, and its solution is $D(t) = D_0 e^{-kt}$, where D_0 is the initial drug concentration.

2 Analysis of the system

2.1 Existence and properties of solution

In this section, we study the existence, uniqueness, positivity and boundedness of the solution of system of equations (1.16)-(1.21).

Proposition 2.1. *For any non-negative initial condition $(A(0), u(0), M_1(0), M_2(0), C_1(0), C_2(0))$, the system (1.16)-(1.21) has a unique global solution which is bounded.*

Proof. Existence and uniqueness of a local solution directly follows from the Cauchy–Lipschitz theorem for ordinary differential equations.

The solution is bounded because from the fifth equation of system (1.16)-(1.21), we conclude that if $M_2(t)$ is large enough then $\frac{dM_2}{dt} < 0$ and, therefore, M_2 remains bounded. By reapplying the same argument, we subsequently conclude the same result for the rest of the variables of the system. Since the solutions of system (1.16)-(1.21) are bounded, they are defined for all $t > 0$. □

Proposition 2.2. *From Proposition 2.1 in [40], for any positive initial condition, the solution of the system (1.16)-(1.21) is positive.*

Proof. Consider the vector field $F = (f_1, ..., f_6)$ for $x = (x_1, ..., x_6) \in \mathbb{R}^6$ given by

$$\begin{cases} f_1(x) = k_1 x_4 N - 2k_2 x_1^2 - \sigma_1 x_1, \\ f_2(x) = k_2 x_1^2 - \sigma_2 x_2(1 + bx_5), \\ f_3(x) = k_3 x_2(M_1^0 - x_3) - \sigma_3 x_3, \\ f_4(x) = \frac{k_4 x_3}{(1+k_5 x_6)(1+aD)} - \sigma_4 x_4, \\ f_5(x) = k_6 x_2(M_2^0 - x_5) - \sigma_5 x_5, \\ f_6(x) = k_7 x_5 - \sigma_6 x_6, \end{cases}$$

and observe that F satisfies the quasi-positivity property, that is, for all indices $i \in \{1, ..., 6\}$ we have

$$\text{for all } (x_j)_{j \neq i} \in (\mathbb{R}^+)^5,\ f_i(x_1, ..., x_{i-1}, 0, x_{i+1}, ..., x_6) \geq 0.$$

Hence, from Proposition 2.1 in [40], we conclude that the solution remains positive because of this property. □

2.2 Equilibrium points of the complete model

In order to study the steady states, we let $D(t) = 0$ and find the stationary points of the following system:

$$k_1 C_1 N - 2k_2 A^2 - \sigma_1 A = 0, \tag{2.1}$$
$$k_2 A^2 - \sigma_2 u(1 + bM_2) = 0, \tag{2.2}$$
$$k_3 u(M_1^0 - M_1) - \sigma_3 M_1 = 0, \tag{2.3}$$
$$k_6 u(M_2^0 - M_2) - \sigma_5 M_2 = 0, \tag{2.4}$$
$$\frac{k_4 M_1}{(1 + k_5 C_2)} - \sigma_4 C_1 = 0, \tag{2.5}$$
$$k_7 M_2 - \sigma_6 C_2 = 0. \tag{2.6}$$

From equation (2.1), we get

$$A = A(C_1) = \frac{\left(-\sigma_1 + \sqrt{\sigma_1^2 + 8k_1 k_2 C_1 N}\right)}{4k_2}.$$

From equations (2.2) and (2.4), we write two formulas for u, namely

$$\begin{cases} u := g_1(C_1, M_2) = \dfrac{1}{\sigma_2} \dfrac{k_2 A^2}{bM_2 + 1}, \\ u := g_2(M_2) = \dfrac{\sigma_5 M_2}{k_6(M_2^0 - M_2)}. \end{cases} \tag{2.7}$$

Equating both equations of system (2.7), we express M_2 in terms of C_1:

$$M_2 = \frac{-\left(\sigma_5\sigma_2 + k_2 k_6 A^2\right) + \sqrt{\left(\sigma_5\sigma_2 + k_2 k_6 A^2\right)^2 + 4\sigma_5\sigma_2 b\left(k_2 k_6 A^2 M_2^{0\,2}\right)}}{2\sigma_5\sigma_2 b}.$$

Similarly, we express u, C_2 and M_1 in terms of C_1 from equations (2.2), (2.6) and (2.3), respectively:

$$u = \frac{k_2 A^2}{\sigma_1(1 + bM_2)} = \frac{2k_2\sigma_5 A^2}{\sigma_2\sigma_5 - k_2 k_6 A^2 + \sqrt{\left(\sigma_5\sigma_2 + k_2 k_6 A^2\right)^2 + 4\sigma_5\sigma_2 b\left(k_2 k_6 A^2 M_2^{0\,2}\right)}},$$

$$C_2 = \frac{k_7}{\sigma_6} M_2,$$

$$M_1 = \frac{k_3 u M_1^0}{k_3 u + \sigma_3} = \frac{2\sigma_5 k_2 k_3 A^2 M_0^1}{\sigma_3\left(\sigma_2\sigma_5 - k_6 k_2 A^2 + \sqrt{\left(\sigma_5\sigma_2 + k_2 k_6 A^2\right)^2 + 4\sigma_5\sigma_2 b\left(k_2 k_6 A^2 M_2^{0\,2}\right)}\right) + 2k_3 k_2 \sigma_5 A^2}.$$

Replacing those expression in equation (2.5), we get the following expression in terms of C_1:

$$\frac{k_4 M_1(C_1)}{1 + k_5 C_2(C_1)} = \sigma_4 C_1.$$

We obtain that the trivial equilibrium point $E_0 = (0, 0, 0, 0, 0, 0)$ exists for all values of parameters. The computation of the solution with respect to C_1 are too tedious. Hence, we suggest a geometrical perspective in order to find the number of non-negative steady states. We define the functions

$$f_1(C_1) = \frac{k_4 M_1(C_1)}{1 + k_5 C_2(C_1)}, \qquad f_2(C_1) = \sigma_4 C_1.$$

The curves f_1 and f_2 have up to three intersection where $C_1 \geq 0$ (see Figure 2a).

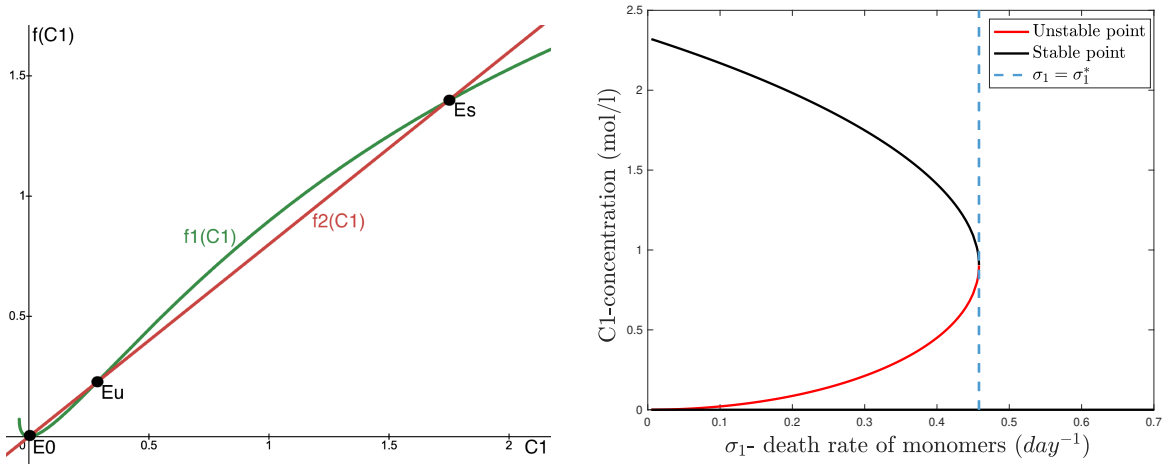

(a) Equilibrium points in the bistable case.

(b) Bifurcation diagram C_1 vs σ_1

Figure 2: Existence and stability of equilibrium points. Figure 2a represents the bistable case where three equilibrium points exist E_0, E_u and E_s, with $\sigma_4 = 1.2$. Figure 2b represents a bifurcation diagram of the equilibrium points for the concentration of pro-inflammatory cytokines C_1 in terms of the degradation rate σ_1 of monomers (Aβ). The disease-free equilibrium exists for all values of $\sigma_1 > 0$ and it is stable. For $\sigma_1 < \sigma_1^*$, we have two other equilibrium points E_u unstable (red line) and E_s stable (black line). Values of parameters are taken from Table 2.

We conclude that system (2.1)-(2.6) may end up with a total of three positive equilibrium points, namely E_0, E_u and E_s.The case with only one equilibrium point E_0 corresponds to the non-inflammatory case. The bistable case is depicted in Figure 2(a) and is represented by the existence of three equilibrium points E_0, E_u and E_s. Another classification of the equilibrium points, based on the parameter σ_1, is presented in Section 2.3.

2.3 Stability of equilibrium points

Proposition 2.3. *For the system (1.16)-(1.21), the disease-free equilibrium $E_0 = (0, 0, 0, 0, 0, 0)$ is stable for every choice of positive parameters.*

Proof. The Jacobian matrix around the vector $(0,0,0,0,0,0)$ is given by

$$J = \begin{pmatrix} -\sigma_1 & 0 & 0 & 0 & k_1 N & 0 \\ 0 & -\sigma_2 & 0 & 0 & 0 & 0 \\ 0 & k_3 M_1^0 & -\sigma_3 & 0 & 0 & 0 \\ 0 & k_6 M_2^0 & 0 & -\sigma_5 & 0 & 0 \\ 0 & 0 & k_4 & 0 & -\sigma_4 & 0 \\ 0 & 0 & 0 & k_7 & 0 & -\sigma_6 \end{pmatrix}.$$

The eigenvalues of this matrix are $\{-\sigma_1, -\sigma_2, -\sigma_3, -\sigma_4, -\sigma_5, -\sigma_6\}$. Since they are all negative, then the disease-free equilibrium is locally asymptotically stable. □

We determine the stability of the equilibrium points E_u and E_s using numerical simulations, as shown in Figure 2(b). We perform a bifurcation analysis with respect to the variation of the parameter σ_1, where we consider the C_1-coordinate of the equilibrium points. Numerical simulations show that there are two different cases depending on the parameter σ_1:

- If $\sigma_1 > \sigma_1^*$, there is a single point E_0, AD does not develop and we denote this case by disease-free case.
- If $\sigma_1 < \sigma_1^*$, there are three points (E_0, E_u, E_s), AD develops if the initial perturbation (inflammation) is sufficiently large. We denote this case by bistable case.

2.4 Biological interpretation

In this section, we provide a biological interpretation of the equilibrium points.

- E_0 corresponds to the non-inflammatory state where all concentrations are zeros. In other words, there are no oligomers, immune cells or inflammatory cytokines. Thus, there is no interaction between inflammatory agents; hence, no inflammation reaction can happen in this case. This point exists for all values of parameters and is stable.
- E_u is an intermediate equilibrium point, it is unstable whenever it exists. Indeed, it represents a threshold to overcome in order to move from the non-inflammatory state E_0 to the inflammatory state E_s.
- E_s represents an inflammatory state. All inflammatory agents and key-players of AD have positive concentrations. This point characterizes the set-up of AD along with an inflammatory reaction. Therefore, E_s characterizes the disease state and is stable whenever it exists.

We study then the development of the disease in the bistable case (existence of three equilibrium points). We are interested in showing how NSAID affects the dynamics of the solution and whether it can limit or reverse the development of the disease at an early stage. Since the study of the system of equations (1.1)-(1.9) is analytically challenging, we begin with a simplified model in order to illustrate the method of analysis and the main results. Then we apply this method to the complete model.

3 Simplified model

In this section, we derive a simplified model in order to study the dynamics of the solution. We assume that the concentration of Aβ-monomers A is sufficiently small and neglect then the term A^2 with respect to A in equation (2.1). Then $A = a_1 C_1$, where $a_1 = k_1 N/\sigma_1$. From equation (2.4) we conclude that for when concentrations of M2 type microglia M_2 is small, it is considered proportional to u (concentration of oligomers): $M_2 = a_4 u$, where $a_4 = k_6 M_2^0/\sigma_5$. Hence, equation (2.2) is rewritten as:

$$k_2 A^2 - \sigma_2 b a_4 u^2 - \sigma_2 u = 0, \tag{3.1}$$

Neglecting the term u^2 compared to the term u in equation (3.1), we get $u = a_2 A^2$, where $a_2 = k_2/\sigma_2$. Next, from equation (2.3) we write: $M_1 = a_3$, where $a_3 = k_3 M_1^0/\sigma_3$, and from equation (2.6), $C_2 = a_5 M_2$, where $a_5 = k_7/\sigma_6$. Substituting these expressions into equation (2.5), we obtain the following equation with respect to C_1:

$$\frac{C_1^2}{(1+\alpha C_1^2)} = \gamma C_1, \tag{3.2}$$

where

$$\alpha = a_1^2 a_2 a_4 a_5 k_5, \quad \gamma = \frac{\sigma_4}{a_1^2 a_2 a_3 k_4}.$$

Equation (3.2) has solution $C_1 = 0$ and, depending on parameters, up to two positive solutions denoted by $C_1^{(1)}$ and $C_1^{(2)}$, $C_1^{(1)} < C_1^{(2)}$.

- If $\Delta = 1 - 4\alpha\gamma^2 < 0$, there exists only one stationary solution $C_1 = 0$.
- If $\Delta = 1 - 4\alpha\gamma^2 > 0$, there exist three stationary solutions $C_1 = 0$, $C_1^{(1)} = \frac{1-\sqrt{\Delta}}{2\alpha\gamma}$ and $C_1^{(2)} = \frac{1+\sqrt{\Delta}}{2\alpha\gamma}$.

Thus, under the simplifying assumptions formulated above (small concentrations), system (1.16)-(1.21) has a zero stationary point P_0 and up to two positive stationary points P_1 and P_2. In terms of stability analysis, P_0 and P_2 are stable whereas P_1 is unstable.

3.1 Formulation of the model problem

Let us consider the time-dependent simplified equation obtained from system (1.16)-(1.21) similar to (3.2) under the quasi-stationary approximation for all variables except for C_1:

$$\frac{dC_1}{dt} = \frac{C_1^2}{(1+\alpha C_1^2)(1+aD(t))} - \gamma C_1. \tag{3.3}$$

Here we take into account down-regulation of the rate of inflammatory cytokine production by NSAID with time-dependent concentration $D(t)$ described by the equation $D(t) = D_0 e^{-kt}$, where D_0 is the initial drug concentration. For $D = 0$, stationary solutions of equation (3.3) are provided by equation (3.2).

By linearizing equation (3.3) about the intermediate stationary point, we obtain a linear equation with time-dependent coefficients. This time dependence changes the position of the intermediate point in such a way that its value increases for larger D. We preserve this property in the model problem

$$\frac{du}{dt} = a(u - u_1(t)) - bu, \tag{3.4}$$

where $u_1(t) = (1 + D(t))\, u_0$, $u(0) = u_*$. This linear equation has a similar behavior in the vicinity of the intermediate zero of the right-hand side as equation (3.3). We consider this simplified model to determine the properties of the analytical solution.

In order to solve equation (3.4), we write it in the form

$$\frac{du}{dt} = (a-b)u - au_0 - au_0 D_0 e^{-kt}, \tag{3.5}$$

and set $\alpha = a - b, \beta = au_0 D_0$, $v = u - au_0/(a-b)$. We assume here that $a \neq b$. Then

$$\frac{dv}{dt} = \alpha v - \beta e^{-kt}, \quad v(0) = u_* - au_0/(a-b). \tag{3.6}$$

We find

$$v(t) = c_1 e^{\alpha t} + \frac{\beta}{\alpha + k} e^{-kt},$$

where c_1 is determined from the initial condition:

$$c_1 = u_* - \frac{au_0}{a-b} - \frac{\beta}{\alpha + k}\,.$$

Hence

$$u(t) = v(t) + \frac{au_0}{a-b} = \left(u_* - \frac{au_0}{a-b} - \frac{\beta}{\alpha+k}\right) e^{\alpha t} + \frac{\beta}{\alpha+k} e^{-kt} + \frac{au_0}{a-b}\,,$$

or

$$u(t) = (u_* - p - q)\, e^{\alpha t} + q e^{-kt} + p\,,$$

where

$$p = \frac{au_0}{a-b}, \quad q = \frac{\beta}{\alpha+k} = \frac{au_0 D_0}{a-b+k}\,.$$

Properties of solutions. Behavior of solution depends on the values of parameters. There are the following cases:

- If $u_* < \dfrac{au_0}{a-b}$, inflammation decays even without treatment.
- If $\dfrac{au_0}{a-b} < u_* < \dfrac{au_0}{a-b} + \dfrac{\beta}{\alpha+k}$, inflammation decays after the first drug administration.
- If

$$u_* > \frac{au_0}{a-b} + \frac{\beta}{\alpha+k}, \tag{3.7}$$

and $\alpha \left(u_* - \dfrac{au_0}{a-b} - \dfrac{\beta}{\alpha+k}\right) > \dfrac{\beta k}{\alpha+k}$, inflammation grows after the single drug administration. Therefore, it also grows for any further administrations with the same D_0 since the initial condition is larger than the first time.

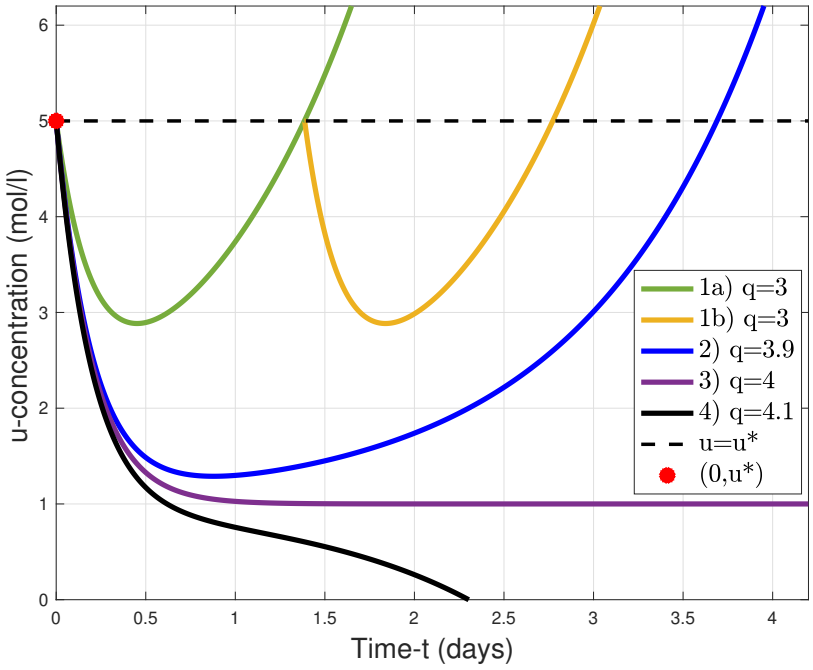

Figure 3: Solutions of equation (3.4) with initial condition $u(0) = u_*$ and single drug administration. The values of parameters: $u_* = 5, p = 1, \alpha = 1, k = 5$, $q = 3$ (curve **1a**), $q = 3.9$ (curve **2**), $q = 4$ (curve **3**), $q = 4.1$ (curve **4**). The curve (curve **1b**) corresponds to the solution with the same values of parameters as (curve **1a**) but shifted in time.

- If (3.7) is satisfied and $\alpha\left(u_* - \dfrac{au_0}{a-b} - \dfrac{\beta}{\alpha+k}\right) < \dfrac{\beta k}{\alpha+k}$, then $u(t)$ first decreases, then grows.

Figure 3 shows the behavior of solution depending on the value of parameter q (proportional to D_0) for all other parameters fixed. If D_0 is sufficiently small, then solution is exponentially growing (not shown). For larger values, the solution first decays, then grows. Finally, if D_0 is large enough, the solution decreases. It becomes negative because we replaced the nonlinear problem by its linear approximation. This approximation is appropriate for the values of solution close to the unstable stationary point. Let us note that for a unique value of q, solution converges to this unstable stationary solution (curve 3). Thus, even a single administration of drug can inverse dynamics of inflammation.

For some intermediate values of D_0, solution decreases after drug administration and begins to grow after some time. In this case, consecutive drug administrations should be applied. We discuss the optimal administration regimen below.

3.2 Optimal drug regimen

We suppose that there are two limitations on drug administration [41, 42]: (a) single drug dose should not exceed some maximal value D_m, (b) total drug dose during some time period T should not exceed the maximal value D_T.

Different treatment regimens can be used. For example, we apply the maximal single dose D_m every time interval τ, or half of this dose $D_m/2$ twice more often. Which of them is theoretically better from the point of view of minimization of solution? We answer this question in the following setting. Consider some given initial condition $u(0) = u_*$. Our aim is to keep the value of solution below this value u_*, that is, prevent inflammation growth. Hence, at the first step of the analysis, we determine the optimal strategy to keep $u(t) \leq u_*$ depending on the value of single dose administration without taking into account the total amount D_T.

Consider a single drug administration (Figure 3, curves 1a and 2) and denote by τ the value of time for which $u(\tau) = u_*$. We call this value τ the return time. We aim to maximize the return time with the same (or smaller) drug dose. Let us begin with the following example: for $q = 3$, we have $\tau \approx 1.4$, and for $q = 3.9$, $\tau \approx 3.7$. Hence, increasing drug dose in $3.9/3 = 1.3$ folds, we increase the time period in $3.7/1.4 \approx 2.6$ folds. Therefore, time increase is larger than the dose increase, and it is more efficient to use the maximum tolerated single dose D_m.

Figure 3 shows the solution for the second drug administration for $q = 3$ at the moment of time when the solution returns to the value u_* at time $t = 1.4$. We see that in this example two consecutive applications of drug dose with $q = 3$ is less efficient than a single drug administration with $q = 3.9$, in the sense that return time is larger. As before, we conclude that the optimal strategy is to use the maximal tolerated single dose D_m.

From the equality $u(\tau) = u_*$ we obtain

$$q = (u_* - p)\frac{1 - e^{-\alpha\tau}}{1 - e^{-(\alpha+k)\tau}} \equiv F(\tau) \ .$$

If τ is increased s times, we can verify that the corresponding increase of q is less than s times, that is,

$$F(s\tau) < sF(\tau), \quad s > 1. \tag{3.8}$$

This means that the increase of a single dose leads to a larger increase of the time interval when the solution returns to the initial value. Therefore, the maximum tolerated single dose provides optimal treatment from the point of view of maximization of return time. Inequality (3.8) is verified numerically in a large parameter range.

4 Anti-inflammatory drugs treatment in the complete model

In this section, we study numerically the complete system of equations (1.16)-(1.21) and we seek to determine optimal regimen using the method presented in Section 3. In numerical simulations, we find the return time as a function of drug dose. Analysis of this function allows us to figure out the regimen maximizing the return time. Values of parameters are taken from Table 2 (Appendix).

4.1 Beginning of inflammation

We consider the initial condition near the unstable equilibrium point E_u, as presented in Table 1. This case characterizes the beginning of inflammation. We retrieve similar solution behavior as presented in Section 3.2. However, the solution converges to equilibrium points E_0 and E_s for larger times, instead of divergence to $\pm\infty$. The numerical time step is considered $\Delta t = 10^{-4}$ and final time of simulations is $T = 200$.

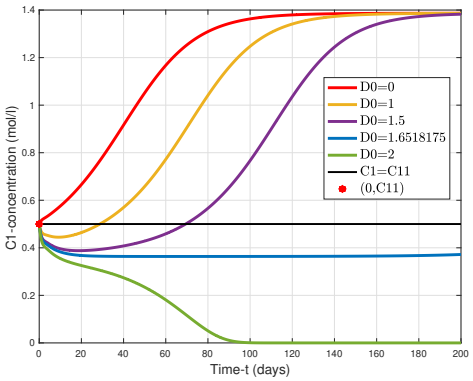

(4a) Solutions of equation (1.16)-(1.21) with initial condition $C_1(0) = C_0 = 0.5$ (black curve) and single drug ad-ministration. The values of the parameter D_0: $D_0 = 0$ (red curve), $D_0 = 1$ (yellow curve), $D_0 = 1.5$ (magenta curve), $D_0 = 1.6518175$ (blue curve), $D_0 = 2$ (green curve).

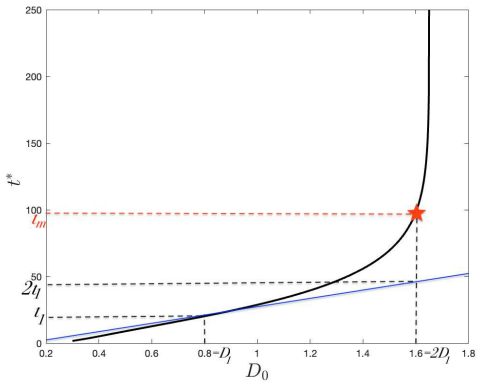

(4b) The return time function F determines the dependence of the return time t^* on the parameter D_0. Denote by t_1 and t_m the return time for the single dose $D_0 = D_1$ and $D_0 = 2D_1$, respectively. Applying two consecutive times the initial dose $D_0 = D_1$, leads to a return time $2t_1 < t_m$.

Figure 4a shows the behavior of solution depending on the value of D_0 for all other parameters fixed. If D_0 is sufficiently small, then solution is exponentially growing (red curve). For intermediate values, the solution first decays, then grows (yellow and magenta curves). Finally, if D_0 is large enough, the solution decreases (green curve). It decays to the $C_1 = 0$ stationary solution. Let us note that for a unique value of D_0, solution converges to this unstable stationary solution (blue curve). The value of such threshold value is obtained via the bracketing method. Thus, even a single administration of drug can inverse dynamics of inflammation. We retrieve a similar solution properties for the remaining concentrations, namely U, A, M_1, M_2 and C_2.

Return time. We fix the initial condition $C_1(0) = 0.5$, as an example, and for the value of $D_0 < 1.66$, the solution first decays due to the effect of the initial dose as shown in Figure 4a (magenta and yellow curves), then grows and reaches after some time the value of the initial concentration $C_1(0)$. We denote by t^* this specific time. We study, through numerical simulations, the dependence of the return time t^* on the value of D_0.

Figure 4b shows that the dependence between the time needed to reach the initial value condition $C_0 = 0.5$ and the value of D_0 is not linear. For values of $D_0 > 1.66$, the solution decays to the zero equilibrium point, hence there is no return time to the initial condition. We have shown for the simplified model that for large enough values of D_0, even a single administration of drug can inverse dynamics of inflammation. A similar case is seen in this case for value of $D_0 > 1.66$. However, for doses $D_0 < 1.66$, inflammation decays then grows until reaching the initial condition at time $t^* > 0$ (this case is seen in Figure 4a for $D_0 = 1$). We notice in Figure 4b that for any value of D, the return time function $F(D)$ satisfies the following condition:

$$F'(D) \geq \frac{F(D)}{D}. \tag{4.1}$$

Condition (4.1) means that any straight line from the origin intersect the curve $F(D)$ only in one point. We show in Section 4.3 that the optimal dose in this case is the maximum tolerated dose.

4.2 Advanced inflammation

Advanced inflammation is considered here as solution essentially larger that the intermediate stationary point. It eventually approaches the stable equilibrium point E_s. Suppose that the initial condition is close to this point, as presented in Table 1. This starting point corresponds to an advanced inflammatory stage. We retrieve a similar solution behavior as presented in Section 4.1.

The solution depends on the value of D_0 for all other parameters fixed. If D_0 is sufficiently small, then solution is exponentially growing. For intermediate values, the solution first decays, then grows. Finally, if D_0 is large enough, the solution decreases. It decays to the $C_1 = 0$ stationary solution. Let us note that for a unique value of D_0, solution converges to this unstable stationary solution. Figure 5a shows the return time function. We note that this function has a concave shape for small D_0 and convex shape for large D_0. Condition (4.1) is not satisfied in this case.

4.3 Optimal drug regimens

In this section, we study the optimal dose by comparing between the two scenarios of initial conditions. A treatment by NSAID should have appropriate dosage and duration [41, 42]. Therefore, we suppose two limitations on drug administration:

A. A single drug dose should not exceed some maximal value denoted by D_m,

B. The total drug dose during some time period T should not exceed the maximal value D_T.

We aim to maximize the return time of the solution to the initial concentration. Let the return time for some dose D_1 be t_1. Then applying consecutively the same dose we obtain the total return time $2t_1$. However, applying single dose $2D_1$, we obtain return time $t_m > 2t_1$ (Figure 4b). For illustration, we let $D_m = 1$, $T = 100$ days and $D_T = 4$. Then a single dose $D_0 = D_m = 1$, does not inverse the dynamics of the solution (Figure 4a) leading to the problem of maximizing the return time t^*. We consider two different initial doses $D_0 = D_m = 1$ and $D_1 = D_m/2 = 0.5$ with their respective return time $t_m = 28$ days and $t_1 = 9$ days. If we apply two consecutive time the same dose D_1, the maximal return time is $2t_1 = 18$ days which is less compared to $t_m = 28$ days. Hence, in order to maximize the return time t^*, we should use the maximal tolerated dose D_m.

For the advanced stage, we denote by D_m the maximum tolerated dose and by D_1 the dose chosen as pictured in Figure 5a and it satisfies the following condition:

$$F'(D) = \frac{F(D)}{D}. \tag{4.2}$$

We note here that applying consecutive time (k times) the dose D_1 has a return time larger than for the maximal tolerated dose, $kt_1 > t_m$, as shown for in Figure 5a.

For illustration, we consider two different values of the administrated drug concentration, the maximum tolerated dose $D_m = 2$ and the value $D_1 = 0.45$. For the initial dose $D_m = 2$, the return time is $t^* = 43$ days, whereas for $D_1 = 0.45$, the return time is $t_1^* = 15$ days.

Under the constraint imposed by condition B, suppose that the total drug dose for a period of 100 days is $D_T = 4$. Hence, for $D_m = 2$, we apply this dose a second time time after 43 days, leading to the maximal return time to be 86 days. In opposition, we apply the same dose $D_1 = 0.45$ in total for eight times with 15 days between two doses and the maximal return time is 120 days. Both cases of consecutive doses are pictured in Figure 5b. We notice that, the optimal dose in this case is not the maximal dose as in case 1, but the dose D_1. The dose D_1 is the value chosen to satisfy condition (4.2). We deduce that for

an advanced stage of the disease, the optimal dose is not the maximum tolerated dose as for the previous case.

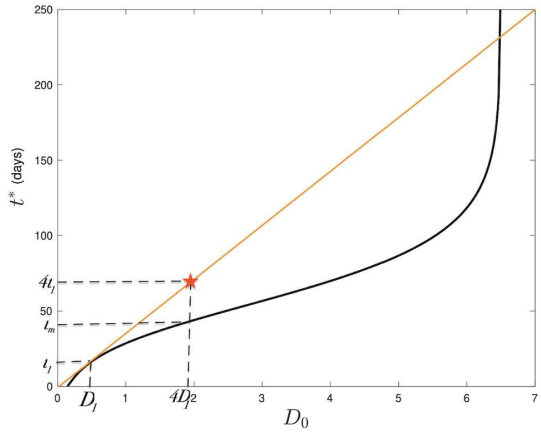

(5a) The function $F(D)$ showing the cross time t^* dependence on the parameter D_0 (black curve). The tangent line to the curve $F(D)$ at the point $(D_1, F(D_1))$ (orange curve). Denote by t_1 and t_m the return time for the single dose $D_0 = D_1$ and $D_0 = 4D_1$, respectively. Applying four consecutive times the initial dose $D_0 = D_1$, leads to a return time $4t_1 > t_m$.

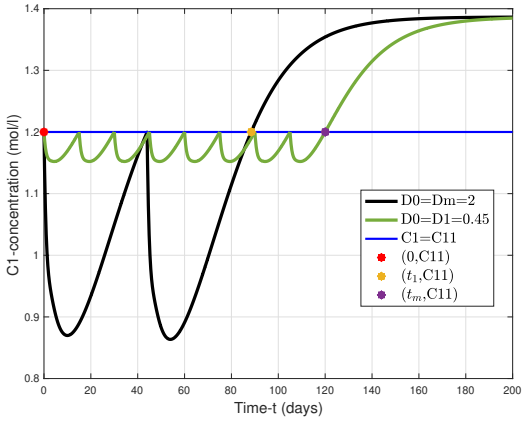

(5b) The solution behavior for the application of consecutive doses of two different small doses: $D_0 = D_1 = 0.45$ (green curve) and $D_0 = D_m = 2$ (black curve). The maximal return time, under condition A and B, are highlighted in dots (purple and yellow, respectively). Consecutive doses of small doses increases the maximal return time.

Consecutive doses. We have shown above how to choose the optimal single dose on the basis of the return time function. This can be the maximum tolerated dose at the initial stage of the disease or a different dose for an advanced stage. At the second stage of this analysis we evaluate the result of treatment taking into account the total admissible dose D_T. Let t^* be the return time for the optimal dose D^*. Applying this dose T/t^* times, we obtain the total dose D^*T/t^* . If

$$D^*T/t^* < D_T, \tag{4.3}$$

that is, the total applied dose is less than the total admissible dose, then we decrease the time interval between drug administrations to some $t^{**} < t^*$ such that $D^*T/t^{**} = D_T$. After the first drug administration, the concentration of inflammatory cytokines $C_1(t^{**})$ is less than the initial concentration $C_1(0) = C_1(t^*)$. Similarly, after each next drug administration the concentration decreases in comparison with the previous administration. Thus, in this treatment protocol inflammation gradually decreases.

At the end of treatment, after T/t^{**} drug administrations, solution of problem (1.16)-(1.21) returns to the basin of attraction of the inflammation-free stationary point. In this case, treatment can be stopped, and inflammation will gradually disappear. If the solution remains in the basin of attraction of of the endemic stationary point, then without treatment inflammation will restart. If inequality (4.3) is opposite, then the time interval between administrations should be increased to some $t^{\#}$ such that $D^mT/t^{\#} = D_T$. In this case, after the first drug administration the concentration of inflammatory cytokines will exceed the initial concentration, $C_1(t^{\#}) > C_1(t^*) = C_1(0)$. After each next administration, the concentration will be larger compared to the previous administration, and the concentration will grow. In this case, treatment cannot eliminate inflammation but it slows it down. After the end of treatment, inflammation will accelerate.

For illustration, we consider the advanced inflammation stage with $D_m = 1$ and $T = 100$ days. We consider that each administered dose is the maximum tolerated dose ($D_0 = D_m = 1$). Figure 6 shows five different cases for the value of D_T. The case $D_T = 1$ means that only a maximal dose of $D_0 = 1$ can be administered in 100 days. We note that the solution decays then grows, reaches the initial condition value for $t^* = 28$ days and converges to the stable point E_s. For $D_T = 4$, we apply four times the single dose $D_0 = 1$ with a time interval of 28 days between the two doses and the final return time is $t^* = 112$ days. For larger values of D_T, we increase the frequency of doses so that the time between two administration is less than the return time. Figure 6 shows that for $D_T = 14$, we apply 14 consecutive doses (each dose of $D_0 = 1$) with an interval of 7 days between two consecutive ones. Under such dose administration, the solution decays, overcomes the threshold (concentration of the unstable equilibrium point E_u) and converges to the zero-equilibrium point E_0. Hence, increasing the frequency of doses can lead to stop the development of the disease.

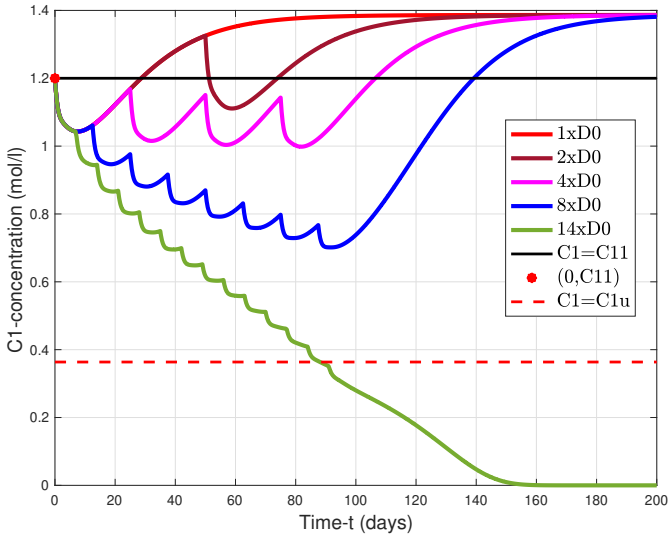

Figure 6: Solutions of equation (1.16)-(1.21) with initial condition $C_1(0) = C_0 = 1.2$ (black curve) and consecutive drug administration for $D_T = 1$ (red curve), $D_T = 2$ (burgundy curve), $D_T = 4$ (magenta curve), $D_T = 8$ (blue curve) and $D_T = 14$ (green curve). The red dash line corresponds to the C_1-concentration of the unstable point E_u.

4.4 Efficiency of anti-inflammatory drugs treatment

We discuss here why the NSAID treatment appears more efficient at early stages of the disease. We consider the effect of initial conditions on the disease development after a treatment of consecutive doses. Once the treatment is administered, the solution decays until reaching time t_{Fend}, indicating the end of the treatment. After this stage, for $t > t^{Fend}$, the solution of problem (1.16)-(1.21) returns to the basin of attraction of the inflammation-free stationary point. In this case, treatment can be stopped, and inflammation will gradually disappear. If the solution remains in the basin of attraction of the endemic stationary point, then without treatment inflammation restarts and grows until reaching the endemic stable point E_s.

For illustration, we consider the administration of five consecutive doses of $D_0 = 1$ with 20 days of gap between two successive doses. Figure 7a shows that for small initial conditions, the treatment is sufficient to decay the concentration of inflammatory cytokines to zero. In opposition, for large initial conditions, the solution grows once the treatment ends and converges to the stable equilibrium point E_s. Thus, the proposed treatment can inverse dynamics of inflammation at the early stage of the disease, but not in an advanced inflammatory stage. We note that the solution for the early stage of the disease (green curve) reaches the basin of attraction of the inflammation-free stationary point after the administration of the third dose. Hence, the treatment could be stopped without the application of the last two doses.

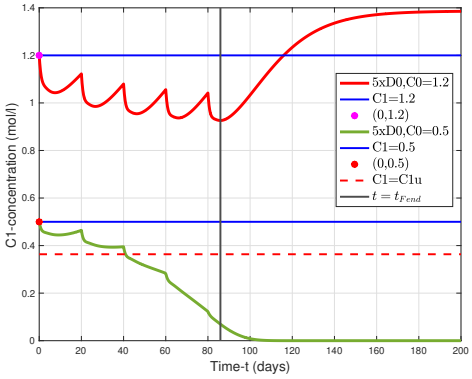

(7a) Solutions of equation (1.16)-(1.21) with five consecutive doses (20 days between doses of $D_0 = 1$) and initial conditions: $C_0 = 0.5$ (green curve) and $C_0 = 1.2$ (red curve). The red dash line corresponds to the C_1-concentration of the unstable point E_u. The vertical black line represents the time where the NSAIDs treatment ends.

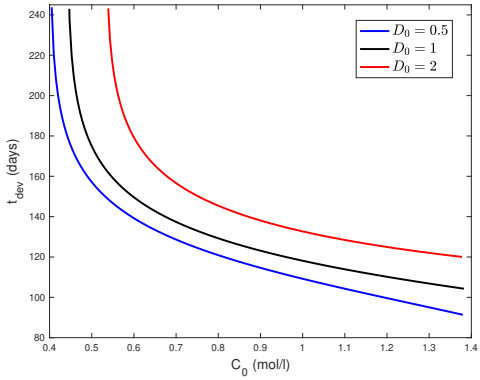

(7b) The disease development time t_{dev} dependence on the initial condition C_0 for three different values of a single dose administration: $D_0 = 0.5$ (blue curve), $D_0 = 1$ (black curve) and $D_0 = 2$ (red curve). We consider values of C_0 between the C_1-concentrations of the unstable point E_u and the stable point E_s.

We denote by t_{dev} the time needed for the solution to reach the vicinity of the point E_s. In other words, t_{dev} represents the time needed for the development of the disease. We study the dependence of the disease development time t_{dev} with respect to the initial condition of inflammatory cytokines C_0. Figure 7b shows that for the same single dose administration D_0, the disease takes more time to develop for larger initial conditions. Such case corresponds to advanced stages of the disease. In contrast, at early stages of the disease, a single dose can delay its development for larger period of time. Therefore, NSAIDs treatment is more efficient at early stages of the disease. Note that this has been observed in [25] which reinforce this theoretical work.

5 Discussion

The main objective of this work is to model the effect of NSAIDs on the progression of the Alzheimer disease. We develop a model describing the interaction of amyloid-β production and inflammation, and show that the NSAID treatment can delay the inflammation progression or even completely suppress it. The result of treatment depends on many factors, such as patient-specific parameters of the model, the stage of the disease advancement, the choice of optimal treatment regimen. The primary objective of this work is to explore how different parameters influence the qualitative behavior of the system and to identify potential mechanisms that need further experimental investigation. Although the modeling

approach is simplified, it offers a valuable perspective and can help to formulate hypotheses and guide future research. These modelling results can give some additional insight on the discrepancy between epidemiological and clinical studies on the effect of NSAID treatment in the Alzheimer disease [25, 30].

Biological evidences. This work validates several biological evidences of NSAID efficacy such as the dose-dependent behavior, the effect of treatment frequency, and the stage-dependent efficacy of the intervention. The simulations presented in Figures 4a, 6, and 7a capture major role of NSAID on the development of inflammation in AD. Figure 4a demonstrates the dose-dependent suppression of pro-inflammatory cytokines, consistent with the inhibitory effects of this type of drugs [43]. Figure 6 highlights the importance of treatment frequency, showing that more frequent dosing drives the system toward an inflammation-free equilibrium, in line with cumulative pharmacological effects [44]. Figure 7a pinpoints stage-dependent efficacy, as NSAID treatment effectively reverses inflammation when applied at early stages but is largely ineffective at advanced stages [26]. Therefore, these results support clinical observations and highlight the role of both dose and timing in optimizing anti-inflammatory therapies.

Return time and single dose choice. The choice of the optimal treatment regimen is one of the main questions in the application of NSAID for all inflammatory diseases. We develop in this work a new approach to this question and illustrate it on the model of the Alzheimer disease, but it is also applicable for other diseases.

We define the optimal treatment as a regimen which minimizes the concentration of inflammatory cytokines after some given time interval T under the constraints that a single drug dose cannot exceed some maximum tolerated dose (MTD) and the cumulative drug dose during the time interval T is limited by the total admissible dose.

The approach suggested in this work is different in comparison with conventional optimal control problem. The determination of optimal treatment regimen developed here is based on the notion of return time defined as follows. After a single drug administration, the concentration of inflammatory cytokines can initially decrease, but later it grows again due to drug elimination from the organism. After some time it returns to its initial level observed before the drug administration. This time interval when the concentration of inflammatory cytokines returns to the initial level after a single drug administration is called return time.

The value of return time t_r depends on the parameters of the model, on the initial condition, and on the drug dose. For fixed values of parameters and initial conditions, return time can be considered as a function of the drug dose D, that is, $t_r = F(D)$. The properties of this functions determine the optimal treatment regimen.

Suppose, for instance, that the single drug dose is twice larger, that is $2D$ instead of D. If the return time $F(2D)$ in this case is twice or more larger than $F(D)$, then one single dose $2D$ has advantage in comparison with two consecutive applications of the dose D.

Hence, we can compare the effect of treatment for different drug doses. There is a simple geometrical condition which allows us to determine the regimen which maximizes the return time. If any straight line from the origin, regardless of its slope, intersects the curve $F(D)$ at a single point (Figure 4b), then a larger dose has advantage over a smaller dose (with the same total drug quantity) from the point of view of maximization of the return time. In the analytical form, this condition is given by (4.1). Thus, if this condition is satisfied, then drug should be administrated by MTD. If condition (4.1) is not satisfied, that is, if for some slopes the straight line intersects the curve $F(D)$ at more than one point (Figure 5a), then the optimal value D changes. Indeed, the optimal single dose is provided by the value of D where the

straight line is tangent to the curve $F(D)$ (Figure 5a). Moreover, the optimal dose D is the first point where $F(D)$ satisfies the optimality condition (4.2).

Optimal treatment. Once we have determined the optimal single dose, which maximizes the return time, we are able to identify the optimal regimen during a given time interval T. Let t_r be the return time for the optimal single dose. Administration of this dose every t_r time interval keeps the level of inflammatory cytokines close to the initial value. It does not grow but does not decrease neither. A more frequent administration of the same dose decreases the concentration of inflammatory cytokines, while less frequent administration leads to its growth.

The frequency of drug administration is determined by the total admissible dose D_T. If total dose DT/t_r with the return time frequency is less than D_T, then the frequency can be increased, if $DT/t_r > D_T$, then it should be decreased. The maximal administration frequency is determined from the condition that the total dose administrated during time interval T equals the total admissible dose.

Thus, the most efficient treatment is provided by the optimal single dose and the maximal frequency of administration. Depending on patient-specific parameters of the model and on the initial condition (patients status at the beginning of treatment), the most efficient treatment can have three different outcomes:

- Treatment decreases the level of inflammatory cytokines. At the end of treatment, the concentrations of all involved factors belong to the basin of attraction of the inflammation-free equilibrium. After the end of treatment, inflammation gradually disappears.
- Treatment decreases the level of inflammatory cytokines. At the end of treatment, the concentrations of all involved factors belong to the basin of attraction of the inflammatory equilibrium. After the end of treatment, inflammation continues to amplify.
- Treatment can slow down inflammation progression but it cannot stop its growth.

Other formulations of the optimization problem. Solution of the optimization problem discussed above allows us to minimize the level of inflammatory cytokines at the end of some given time interval under the constraints of maximum tolerated dose and total admissible dose. Another possible formulation of the optimization problem consists in the minimization of total administrated dose for the inflammation suppression under the constraint of maximum tolerate dose. As previously, we consider the optimal single dose maximizing the return time. If the frequency of administration exceeds the return time frequency, then the level of inflammatory cytokines gradually decreases and eventually reaches the basin of attraction of the inflammation-free equilibrium. The total time of treatment and the administration frequency can be assessed in numerical modelling with patient-specific parameters and initial conditions.

The role of disease stage. The stage of the disease progression correlates in the model with the level of inflammatory cytokines at the moment of the beginning of treatment. Smaller initial condition corresponds to the early stage of the disease, while larger initial condition to a more advanced stage. Disease stage determines the optimal single dose and treatment outcome.

We show in this work that optimal single dose maximizing the return time is the MTD in the beginning of the disease progression when the initial condition is close to the unstable equilibrium separating the two stable ones, inflammation-free stationary point and inflammatory stationary point. In opposition, if the initial concentration of all agents key-player is larger, the MTD may not the optimal dose, as presented in Section 4.3.

Next, along with disease progression (concentration of inflammatory cytokines at the beginning of treatment becomes larger), the value of return time decreases. Therefore, more frequent drug administration is required to restrain inflammation progression. For a given total admissible dose, this means that treatment is more efficient in the beginning of the disease. Epidemiological studies support that (NSAIDs) can reduce the disease development if they are started well before clinical signs develop and that a daily dose can be helpful [45]. On the other hand, clinical studies show that NSAID are non-effective in advanced stages of the disease [46, 47]. Hence, this work offers a perspective by bridging the gap between epidemiological and clinical studies. These results support the idea that NSAIDs efficacy in AD is stage-dependent, with early intervention being more beneficial.

Maximum tolerated dose in pharmacology. In pharmacology, the maximum tolerated dose (MTD) refers to the highest dose of a drug or treatment that does not cause unacceptable side effects in patients. It represents the upper limit of drug administration where the therapeutic benefit can be achieved with manageable or minimal adverse effects.

MTD is established during preclinical studies (animal testing) and Phase 1 clinical trials in humans. Doses are gradually escalated to identify the highest level that can be tolerated without severe toxicity. Long-term studies may assess the potential for chronic toxicity at or below the MTD. MTD is essential for optimizing drug dosing regimens, minimizing risks, and ensuring patient safety during therapeutic interventions. For example, the standard clinical practice used for cancer patients is the MTD [48, 49]. This work provides the theoretical conditions under which the maximal dose is the optimal choice (condition (4.1)). The results obtained coincide with clinical strategies used in the treatment of other diseases, where the maximal dose is administrated.

Using MTD is largely discussed in the pharmacological literature (see the review in [50]) but its application is empirical and it is often contested. This work provides a theoretical framework for the assessment of the optimal dose, which can be MTD or different from it.

Limitations and perspectives. The model developed in this work is necessarily simplified. More detailed models taking into account pharmacokinetics of NSAIDs can provide efficacy assessment of specific anti-inflammatory drugs. Further important limitation of such studies is related the estimation of patient-specific parameters. Due to the lack of available biological data, particularly in the early phases of AD, it is challenging to approximate the model parameters. Although the choice of parameters is not patient based, we provided some quantitative conclusions that are independent of specific parameter values.

Medical evidence supports that the use of NSAID can cause additional health complications such as an increase of the blood pressure [51] or kidney damage [52]. Therefore, instead of maximum tolerated dose and total admissible dose it may be appropriate to consider dose-dependent side effects.

A possible extension of this work is to consider the penetration of drugs in the brain from blood, which can lead to several optimal control problems in order to optimize both the time and the amount of dose administered [53]. Another question concerns the effect of diet and food on the development of AD. Several types of diets have been considered as nonpharmacological risk modifying factors for AD [54]. Hence, incorporating the role of diet, having anti-inflammatory characteristics, appears as a promising therapeutic approach for future research. Studies have shown that some drugs known as glucagon-like peptide-1 receptor agonists (GLP-1 RAs) used for type 2 diabetes patients significantly reduce neuroinflammation and the risk of Alzheimer's disease [55, 56].

6 Conclusions

In this work we determine the most efficient protocol of NSAID treatment which allows the minimization of the concentration of inflammatory cytokines at the end of treatment. It is based on the notion of return time, optimal single dose, and maximal admissible frequency of drug administration.

Though this most efficient protocol is patient-specific, we show that at the early stage of the disease progression it is provided by the maximum tolerated dose based on easily available data, such as patient weight, age, and some others.

Even the most efficient treatment protocol may not be successful from the point of view of inflammation suppression. Treatment outcome depends on the disease stage at the beginning of treatment and patient-specific parameters. These results give some additional insights on the discrepancy between epidemiological and clinical studies of the NSAID treatment in the Alzheimer disease.

Let us also note that the approach developed in this work is potentially applicable for the evaluation of optimal treatment regimen in other diseases.

Acknowledgments

This project has received support from Agence National de la Recherche PrionDiff Project-ANR-21-CE15-0011. The last author has been supported by the RUDN University Strategic Academic Leadership Program.

Conflicts of interest statement

This work does not have any conflicts of interest.

Data Availability

The manuscript has no associated data.

Appendix

In this section, we provide values of parameters and initial conditions employed in numerical simulations. We note that due to the lack of available biological data, particularly in the early phases of AD, it is challenging to approximate the model parameters. Although the choice of parameters is not patient based, we provided some quantitative conclusions that are independent of specific parameter values. The units were taken from previous modeling studies to keep the equations dimensionally consistent [37]. The aim of the arbitrary choice of parameters is to illustrate the analytical results obtained for both the simplified and complete versions of the model.

variable	definition	initial condition 1	initial condition 2
C_1	concentration of pro-inflammatory cytokines	$0.5\ \text{mol} \times \text{l}^{-1}$	$1.2\ \text{mol} \times \text{l}^{-1}$
C_2	concentration of anti-inflammatory cytokines	$0.048397\ \text{mol} \times \text{l}^{-1}$	$0.1326065\ \text{mol} \times \text{l}^{-1}$
M_1	concentration of M1 type macrophages	$0.11227\ \text{mol} \times \text{l}^{-1}$	$0.2658713\ \text{mol} \times \text{l}^{-1}$
M_2	concentration of M2 type macrophages	$0.0241986\ \text{mol} \times \text{l}^{-1}$	$0.066303\ \text{mol} \times \text{l}^{-1}$
A	concentration of Aβ-monomers	$0.3064\ \text{mol} \times \text{l}^{-1}$	$0.5264593\ \text{mol} \times \text{l}^{-1}$
u	concentration of oligomers	$0.070263\ \text{mol} \times \text{l}^{-1}$	$0.2011995\ \text{mol} \times \text{l}^{-1}$

`Table 1:` Initial data for the concentration of all variables considered in numerical simulations. Concentration units are taken from [37].

variable	value	units	description
k_1	0.5	$\text{l} \times \text{mol}^{-1} \times \text{day}^{-1}$	production rate of monomers by activated neurons
k_2	0.75	$\text{l} \times \text{mol}^{-1} \times \text{day}^{-1}$	polymerization rate of monomers attaching to oligomers
k_3	0.9	$\text{l} \times \text{mol}^{-1} \times \text{day}^{-1}$	growth coefficient of M1 microglial cells
k_4	4	day^{-1}	growth coefficient of C1 cytokines by M1 microglial cells
k_5	0.1	$\text{l} \times \text{mol}^{-1}$	inhibition of rate in the production of C1 cytokines by C2 cytokines
k_6	0.3	$\text{l} \times \text{mol}^{-1} \times \text{day}^{-1}$	growth coefficient of M2 microglial cells
k_7	1	day^{-1}	production rate of C2 cytokines by M2 microglial cells
k	0.15	day^{-1}	decay rate of the injection dose
a	0.2	$\text{ml} \times \text{mg}^{-1}$	growth coefficient of the dose
D_0	variable	$\text{mg} \times \text{ml}^{-1}$	dose injected of NSAID
M_1^0	1	$\text{mol} \times \text{l}^{-1}$	initial concentration of M1 microglial cells
M_2^0	1	$\text{mol} \times \text{l}^{-1}$	initial concentration of M2 microglial cells
σ_1	0.35	day^{-1}	degradation rate of monomers
σ_2	1	day^{-1}	degradation rate of oligomers
σ_3	0.5	day^{-1}	degradation rate of M1 microglial cells
σ_4	0.8	day^{-1}	degradation rate of pro-inflammatory cytokines
σ_5	0.8	day^{-1}	degradation rate of M2 microglial cells
σ_6	0.5	day^{-1}	degradation rate of anti-inflammatory cytokines
N	1	$\text{mol} \times \text{l}^{-1}$	initial concentration of neurons
b	0.5	$\text{l} \times \text{mol}^{-1}$	elimination rate of oligomers by M2 microglial cells

`Table 2:` Parameter values for the numerical simulations. The numerical values of the parameters were chosen to reproduce the expected qualitative behavior of the system. Their units were adopted from [37] to ensure dimensional consistency.

References

[1] GBD 2019 Dementia Forecasting Collaborators (2022). *Estimation of the global prevalence of dementia in 2019 and forecasted prevalence in 2050: an analysis for the Global Burden of Disease Study 2019.* The Lancet. Public health, 7(2), e105–e125. https://doi.org/10.1016/S2468-2667(21)00249-8.

[2] Cohen, S. I., Linse, S., Luheshi, L. M., Hellstrand, E., White, D. A., Rajah, L., Otzen, D. E., Vendruscolo, M., Dobson, C. M., & Knowles, T. P. (2013). *Proliferation of amyloid-β42 aggregates occurs through a secondary nucleation mechanism.* Proceedings of the National Academy of Sciences of the United States of America, 110(24), 9758–9763. https://doi.org/10.1073/pnas.1218402110.

[3] Sakono, M., & Zako, T. (2010). *Amyloid oligomers: formation and toxicity of Abeta oligomers.* The FEBS journal, 277(6), 1348–1358. https://doi.org/10.1111/j.1742-4658.2010.07568.x.

[4] Sengupta, U., Nilson, A. N., & Kayed, R. (2016). *The Role of Amyloid-β Oligomers in Toxicity, Propagation, and Immunotherapy.* EBioMedicine, 6, 42–49. https://doi.org/10.1016/j.ebiom.2016.03.035.

[5] Jeong, H., Shin, H., Hong, S., & Kim, Y. (2022). *Physiological Roles of Monomeric Amyloid-β and Implications for Alzheimer's Disease Therapeutics.* Experimental neurobiology, 31(2), 65–88. https://doi.org/10.5607/en22004.

[6] Nag, S., Sarkar, B., Bandyopadhyay, A., Sahoo, B., Sreenivasan, V. K., Kombrabail, M., Muralidharan, C., & Maiti, S. (2011). *Nature of the amyloid-beta monomer and the monomer-oligomer equilibrium.* The Journal of biological chemistry, 286(16), 13827–13833. https://doi.org/10.1074/jbc.M110.199885.

[7] Walsh, D. M., & Selkoe, D. J. (2007). *A beta oligomers - a decade of discovery.* Journal of neurochemistry, 101(5), 1172–1184. https://doi.org/10.1111/j.1471-4159.2006.04426.x.

[8] Penke, B., Szűcs, M., & Bogár, F. (2020). *Oligomerization and Conformational Change Turn Monomeric β-Amyloid and Tau Proteins Toxic: Their Role in Alzheimer's Pathogenesis.* Molecules (Basel, Switzerland), 25(7), 1659. https://doi.org/10.3390/molecules25071659.

[9] Kaku, T., Ikebukuro, K., & Tsukakoshi, K. (2024). *Structure of cytotoxic amyloid oligomers generated during disaggregation.* The Journal of Biochemistry, 175(6), 575–585. https://doi.org/10.1093/jb/mvae023.

[10] Hardy, J., & Allsop, D. (1991). *Amyloid deposition as the central event in the aetiology of Alzheimer's disease.* Trends in pharmacological sciences, 12(10), 383–388. https://doi.org/10.1016/0165-6147(91)90609-v.

[11] Hoogland, I. C., Houbolt, C., van Westerloo, D. J., van Gool, W. A., & van de Beek, D. (2015). *Systemic inflammation and microglial activation: systematic review of animal experiments.* Journal of neuroinflammation, 12, 114. https://doi.org/10.1186/s12974-015-0332-6.

[12] Rani, V., Verma, R., Kumar, K., & Chawla, R. (2022). *Role of pro-inflammatory cytokines in Alzheimer's disease and neuroprotective effects of pegylated self-assembled nanoscaffolds.* Current research in pharmacology and drug discovery, 4, 100149. https://doi.org/10.1016/j.crphar.2022.100149.

[13] Douet, V., Tanizaki, N., Franke, A., Li, X., & Chang, L. (2016). *Polymorphism of Kynurenine Pathway-Related Genes, Kynurenic Acid, and Psychopathological Symptoms in HIV.* Journal of neuroimmune pharmacology : the official journal of the Society on NeuroImmune Pharmacology, 11(3), 549–561. https://doi.org/10.1007/s11481-016-9668-7.

[14] Rothhammer, V., & Quintana, F. J. (2015). *Control of autoimmune CNS inflammation by astrocytes.* Seminars in immunopathology, 37(6), 625–638. https://doi.org/10.1007/s00281-015-0515-3.

[15] Guo, S., Wang, H., & Yin, Y. (2022). *Microglia Polarization From M1 to M2 in Neurodegenerative Diseases.* Frontiers in aging neuroscience, 14, 815347. https://doi.org/10.3389/fnagi.2022.815347.

[16] Tang, Y., & Le, W. (2016). *Differential Roles of M1 and M2 Microglia in Neurodegenerative Diseases.* Molecular neurobiology, 53(2), 1181–1194. https://doi.org/10.1007/s12035-014-9070-5.

[17] Su, F., Bai, F., & Zhang, Z. (2016). *Inflammatory Cytokines and Alzheimer's Disease: A Review from the Perspective of Genetic Polymorphisms.* Neuroscience bulletin, 32(5), 469–480. https://doi.org/10.1007/s12264-016-0055-4.

[18] Taipa, R., das Neves, S. P., Sousa, A. L., Fernandes, J., Pinto, C., Correia, A. P., Santos, E., Pinto, P. S., Carneiro, P., Costa, P., Santos, D., Alonso, I., Palha, J., Marques, F., Cavaco, S., & Sousa, N. (2019). *Proinflammatory and anti-inflammatory cytokines in the CSF of patients with Alzheimer's disease and their correlation with cognitive decline.* Neurobiology of aging, 76, 125–132. https://doi.org/10.1016/j.neurobiolaging.2018.12.019.

[19] Janelsins, M. C., Mastrangelo, M. A., Park, K. M., Sudol, K. L., Narrow, W. C., Oddo, S., LaFerla, F. M., Callahan, L. M., Federoff, H. J., & Bowers, W. J. (2008). *Chronic neuron-specific tumor necrosis factor-alpha expression enhances the local inflammatory environment ultimately leading to neuronal death in 3xTg-AD mice.* The American journal of pathology, 173(6), 1768–1782. https://doi.org/10.2353/ajpath.2008.080528.

[20] Tobinick, E., Gross, H., Weinberger, A., & Cohen, H. (2006). *TNF-alpha modulation for treatment of Alzheimer's disease: a 6-month pilot study.* MedGenMed : Medscape general medicine, 8(2), 25.

[21] Kawahara, K., Suenobu, M., Yoshida, A., Koga, K., Hyodo, A., Ohtsuka, H., Kuniyasu, A., Tamamaki, N., Sugimoto, Y., & Nakayama, H. (2012). *Intracerebral microinjection of interleukin-4/interleukin-13 reduces β-amyloid accumulation in the ipsilateral side and improves cognitive deficits in young amyloid precursor protein 23 mice.* Neuroscience, 207, 243–260. https://doi.org/10.1016/j.neuroscience.2012.01.049.

[22] Sastre, M., & Gentleman, S. M. (2010). *NSAIDs: How they Work and their Prospects as Therapeutics in Alzheimer's Disease.* Frontiers in aging neuroscience, 2, 20. https://doi.org/10.3389/fnagi.2010.00020.

[23] Ajmone-Cat, M. A., Bernardo, A., Greco, A., & Minghetti, L. (2010). *Non-Steroidal Anti-Inflammatory Drugs and Brain Inflammation: Effects on Microglial Functions.* Pharmaceuticals (Basel, Switzerland), 3(6), 1949–1965. https://doi.org/10.3390/ph3061949.

[24] Rubio-Perez, J. M., & Morillas-Ruiz, J. M. (2012). *A review: inflammatory process in Alzheimer's disease, role of cytokines.* TheScientificWorldJournal, 2012, 756357. https://doi.org/10.1100/2012/756357.

[25] Rivers-Auty, J., Mather, A. E., Peters, R., Lawrence, C. B., & Brough, D. (2020). *Anti-inflammatories in Alzheimer's disease-potential therapy or spurious correlate?.* Brain communications, 2(2), fcaa109. https://doi.org/10.1093/braincomms/fcaa109.

[26] McGeer, P. L., & McGeer, E. (2018). *Conquering Alzheimer's Disease by Self Treatment.* Journal of Alzheimer's disease : JAD, 64(s1), S361–S363. https://doi.org/10.3233/JAD-179913.

[27] Parepally, J. M., Mandula, H., & Smith, Q. R. (2006). *Brain uptake of nonsteroidal anti-inflammatory drugs: ibuprofen, flurbiprofen, and indomethacin.* Pharmaceutical research, 23(5), 873–881. https://doi.org/10.1007/s11095-006-9905-5.

[28] Sagi, S. A., Weggen, S., Eriksen, J., Golde, T. E., & Koo, E. H. (2003). *The non-cyclooxygenase targets of non-steroidal anti-inflammatory drugs, lipoxygenases, peroxisome proliferator-activated receptor, inhibitor of kappa B kinase, and NF kappa B, do not reduce amyloid beta 42 production.* The Journal of biological chemistry, 278(34), 31825–31830. https://doi.org/10.1074/jbc.M303588200.

[29] Lleo, A., Galea, E., & Sastre, M. (2007). *Molecular targets of non-steroidal anti-inflammatory drugs in neurodegenerative diseases.* Cellular and molecular life sciences : CMLS, 64(11), 1403–1418. https://doi.org/10.1007/s00018-007-6516-1.

[30] Miguel-Álvarez, M., Santos-Lozano, A., Sanchis-Gomar, F., Fiuza-Luces, C., Pareja-Galeano, H., Garatachea, N., & Lucia, A. (2015). *Non-steroidal anti-inflammatory drugs as a treatment for Alzheimer's disease: a systematic review and meta-analysis of treatment effect.* Drugs & aging, 32(2), 139–147. https://doi.org/10.1007/s40266-015-0239-z.

[31] Stewart, W. F., Kawas, C., Corrada, M., & Metter, E. J. (1997). *Risk of Alzheimer's disease and duration of NSAID use.* Neurology, 48(3), 626–632. https://doi.org/10.1212/wnl.48.3.626.

[32] Bertsch, M., Franchi, B., Marcello, N., Tesi, M. C., & Tosin, A. (2017). *Alzheimer's disease: a mathematical model for onset and progression.* Mathematical medicine and biology : a journal of the IMA, 34(2), 193–214. https://doi.org/10.1093/imammb/dqw003.

[33] Helal, M., Hingant, E., Pujo-Menjouet, L., & Webb, G. F. (2014). *Alzheimer's disease: analysis of a mathematical model incorporating the role of prions.* Journal of mathematical biology, 69(5), 1207–1235. https://doi.org/10.1007/s00285-013-0732-0.

[34] Andrade-Restrepo, M., Lemarre, P., Pujo-Menjouet, L., Tine, L., & Ciuperca, S. (2020). *Modeling the spatial propagation of $A\beta$ oligomers in Alzheimer's Disease.* ESAIM: Proceedings and Surveys, 67, 30–45. doi:10.1051/proc/202067003.

[35] Bertsch, M., Franchi, B., Meschini, V., Tesi, M. C., & Tosin, A. (2021). *A sensitivity analysis of a mathematical model for the synergistic interplay of amyloid beta and tau on the dynamics of Alzheimer's disease.* Brain Multiphysics, 2, 100020. doi:10.1016/j.brain.2020.100020.

[36] Puri, I. K., & Li, L. (2010). *Mathematical modeling for the pathogenesis of Alzheimer's disease.* PloS one, 5(12), e15176. https://doi.org/10.1371/journal.pone.0015176.

[37] Ciuperca, I., Pujo-Menjouet, L., Matar-Tine, L., Torres, N., & Volpert, V. (2024). *A qualitative analysis of an $A\beta$-monomer model with inflammation processes for Alzheimer's disease.* Royal Society open science, 11(5), 231536. https://doi.org/10.1098/rsos.231536.

[38] Lee, C., & Friedman, A. (2024). *Generating PET scan patterns in Alzheimer's by a mathematical model.* PloS one, 19(4), e0299637. https://doi.org/10.1371/journal.pone.0299637.

[39] Hao, W., & Friedman, A. (2016). *Mathematical model on Alzheimer's disease.* BMC systems biology, 10(1), 108. https://doi.org/10.1186/s12918-016-0348-2.

[40] Haraux A. 2016 *A simple characterization of positivity preserving semi-linear parabolic systems.* (doi:https://arxiv.org/abs/1610.09909).

[41] Bookstaver, P. B., Miller, A. D., Rudisill, C. N., & Norris, L. B. (2010). *Intravenous ibuprofen: the first injectable product for the treatment of pain and fever.* Journal of pain research, 3, 67–79. https://doi.org/10.2147/jpr.s6993.

[42] Schjerning Olsen, A. M., Fosbøl, E. L., Lindhardsen, J., Folke, F., Charlot, M., Selmer, C., Lamberts, M., Bjerring Olesen, J., Køber, L., Hansen, P. R., Torp-Pedersen, C., & Gislason, G. H. (2011). *Duration of treatment with nonsteroidal anti-inflammatory drugs and impact on risk of death and recurrent myocardial infarction in patients with prior myocardial infarction: a nationwide cohort study.* Circulation, 123(20), 2226–2235. https://doi.org/10.1161/CIRCULATIONAHA.110.004671.

[43] Smith, C. E., Soti, S., Jones, T. A., Nakagawa, A., Xue, D., & Yin, H. (2017). *Non-steroidal Anti-inflammatory Drugs Are Caspase Inhibitors.* Cell chemical biology, 24(3), 281–292. https://doi.org/10.1016/j.chembiol.2017.02.003.

[44] Kelly, T. L., Salter, A., & Pratt, N. L. (2024). *The weighted cumulative exposure method and its application to pharmacoepidemiology: A narrative review.* Pharmacoepidemiology and drug safety, 33(1), e5701. https://doi.org/10.1002/pds.5701.

[45] McGeer, P. L., Guo, J. P., Lee, M., Kennedy, K., & McGeer, E. G. (2018). *Alzheimer's Disease Can Be Spared by Nonsteroidal Anti-Inflammatory Drugs.* Journal of Alzheimer's Disease, 62, 1219–1222. doi:10.3233/JAD-170706.

[46] Imbimbo, B. P., Solfrizzi, V., & Panza, F. (2010). *Are NSAIDs useful to treat Alzheimer's disease or mild cognitive impairment?.* Frontiers in aging neuroscience, 2, 19. https://doi.org/10.3389/fnagi.2010.00019.

[47] Green, R. C., Schneider, L. S., Amato, D. A., Beelen, A. P., Wilcock, G., Swabb, E. A., Zavitz, K. H., & Tarenflurbil Phase 3 Study Group (2009). *Effect of tarenflurbil on cognitive decline and activities of daily living in patients with mild Alzheimer disease: a randomized controlled trial.* JAMA, 302(23), 2557–2564. https://doi.org/10.1001/jama.2009.1866.

[48] Brasky, T. M., Potter, J. D., Kristal, A. R., Patterson, R. E., Peters, U., Asgari, M. M., Thornquist, M. D., & White, E. (2012). *Non-steroidal anti-inflammatory drugs and cancer incidence by sex in the VITamins And Lifestyle (VITAL) cohort.* Cancer causes & control : CCC, 23(3), 431–444. https://doi.org/10.1007/s10552-011-9891-8.

[49] Thun, M. J., Henley, S. J., & Patrono, C. (2002). *Nonsteroidal anti-inflammatory drugs as anticancer agents: mechanistic, pharmacologic, and clinical issues.* Journal of the National Cancer Institute, 94(4), 252–266. https://doi.org/10.1093/jnci/94.4.252/.

[50] Stampfer, H. G., Gabb, G. M., & Dimmitt, S. B. (2019). *Why maximum tolerated dose?.* British journal of clinical pharmacology, 85(10), 2213–2217. https://doi.org/10.1111/bcp.14032.

[51] Brook, R. D., Kramer, M. B., Blaxall, B. C., & Bisognano, J. D. (2000). *Nonsteroidal Anti-Inflammatory Drugs and Hypertension.* Journal of clinical hypertension (Greenwich, Conn.), 2(5), 319–323.

[52] Drożdżal, S., Lechowicz, K., Szostak, B., Rosik, J., Kotfis, K., Machoy-Mokrzyńska, A., Białecka, M., Ciechanowski, K., & Gawrońska-Szklarz, B. (2021). *Kidney damage from nonsteroidal anti-inflammatory drugs-Myth or truth? Review of selected literature.* Pharmacology research & perspectives, 9(4), e00817. https://doi.org/10.1002/prp2.817.

[53] Xiong, Z., Li, X., Ye, M., & Zhang, Q. (2021). *Finite-time stability and optimal control of an impulsive stochastic reaction-diffusion vegetation-water system driven by Lévy process with time-varying delay.* Mathematical biosciences and engineering : MBE, 18(6), 8462–8498. https://doi.org/10.3934/mbe.2021419.

[54] Grant, W. B., & Blake, S. M. (2023). *Diet's Role in Modifying Risk of Alzheimer's Disease: History and Present Understanding.* Journal of Alzheimer's disease : JAD, 96(4), 1353–1382. https://doi.org/10.3233/JAD-230418.

[55] Wang, W., Wang, Q., Qi, X., Gurney, M., Perry, G., Volkow, N. D., Davis, P. B., Kaelber, D. C., & Xu, R. (2024). *Associations of semaglutide with first-time diagnosis of Alzheimer's disease in patients with type 2 diabetes: Target trial emulation using nationwide real-world data in the US.* Alzheimer's & dementia : the journal of the Alzheimer's Association, 20(12), 8661–8672. https://doi.org/10.1002/alz.14313.

[56] Wong, C. K., McLean, B. A., Baggio, L. L., Koehler, J. A., Hammoud, R., Rittig, N., Yabut, J. M., Seeley, R. J., Brown, T. J., & Drucker, D. J. (2024). *Central glucagon-like peptide 1 receptor activation inhibits Toll-like receptor agonist-induced inflammation.* Cell metabolism, 36(1), 130–143.e5. https://doi.org/10.1016/j.cmet.2023.11.009.